J Mater Sci (2018) 53:9690–9700

Energy materials

N-cyanoethyl polyethylenimine as a water-soluble binder for $LiFePO_4$ cathode in lithium-ion batteries

Jinxin Huang[1,2], Jinglun Wang[1], Haoxiang Zhong[1], and Lingzhi Zhang[1,*]

[1] Key Laboratory of Renewable Energy, Guangdong Key Laboratory of New and Renewable Energy Research and Development, Guangzhou Institute of Energy Conversion, Chinese Academy of Sciences, Guangzhou 510640, Guangdong, China
[2] University of Chinese Academy of Sciences, Beijing 100049, China

Received: 31 January 2018
Accepted: 20 March 2018
Published online: 26 March 2018

ABSTRACT

N-cyanoethyl polyethylenimine (CN-PEI) is synthesized by modifying polyethylenimine (PEI) with acrylonitrile through a Michael addition reaction. Depending on cyanoethylation level, CN-PEI can be obtained as a form of solution, micro-emulsion or emulsion in water. CN-PEI micro-emulsion is investigated as water-soluble binder for the application of lithium iron phosphate (LFP) cathode in lithium-ion batteries. CN-PEI binder not only maintains the outstanding dispersion capability of PEI but also exhibits an excellent adhesion strength and higher ionic conductivity because of the introduction of polar cyano groups. As a result, CN-PEI binder can effectively maintain the mechanical integrity and decrease the polarization of LFP electrode during the operation of the battery. LFP electrode with CN-PEI binder exhibits good cycle stability and enhanced rate performance delivering a capacity of 99.6% at a rate of 0.5 C after 100 cycles and a high discharge capacity of 102.4 mAh g^{-1} at 5 C.

Introduction

The binder is an important ingredient in lithium-ion batteries (LIBs), which helps maintain the electrode's physical structure and the whole electrical network integrity and facilitate the transportation of electron and ion [1]. In LIBs industry, polyvinylidene fluoride (PVDF)/N-methyl-2-pyrrolidone (NMP) is commercially applied as a binder system for both positive and negative electrodes because of its excellent binding capability and electrochemical stability [2]. However, NMP is toxic, flammable and explosive which creates severe pollution and safety problems. At elevated temperatures, the exothermic reactions between PVDF and lithiated graphite (Li_xC_6) or metal lithium give rise to thermal runaway leading to safety considerations [3].

Water-soluble binder has been intensively developed to replace PVDF/NMP binder in view of its low cost, high safety and environmental benign features [4, 5]. Carboxymethyl cellulose/styrene–butadiene rubber (CMC/SBR) is successfully used a commercial water-soluble binder for graphite anode [6]. However, the application of water-soluble binder for

Address correspondence to E-mail: lzzhang@ms.giec.ac.cn

https://doi.org/10.1007/s10853-018-2247-y

cathode material is still a big challenge in LIBs industry.

Recently, we have been focusing on the development of water-soluble binders for the application of LIBs. Carboxymethyl chitosan (CCTS) was firstly explored as a water-soluble binder for anode materials (Si, SnS_2) [7, 8] and later extended its challenging use for LFP cathode [9, 10]. LFP prismatic cell (10 Ah) with CCTS/PEDOT:PSS conductive composite binder showed almost comparable cycling performance with the commercial PVDF binder, retaining 89.7% of capacity at 1 C/2 C (charge/discharge) rate over 1000 cycles [10]. To increase the adhesion capability of CCTS, chemically cyanoethylated CCTS (CN-CCTS) was synthesized by introducing polar cyano group in CCTS through a grafting polymerization of acrylonitrile [11]. LFP electrode with CN-CCTS exhibited good resistance to the organic electrolytes and favorable electrochemical kinetics.

Polyethyleneimine (PEI) is a cationic water-soluble polymer with abundant amine groups. It was reported that PEI was used as a dispersing agent to improve the dispersity of LFP in its aqueous slurry [12] and as water-soluble binder for silicon anode [13]. Very recently, Yan et al. reported PEI as a cross-linking binder with hexamethylene diisocyanate (HDI) for lithium–sulfur battery [14]. The amino groups in PEI effectively reduced the polysulfide dissolution, thus leading an improved cycling performance.

In this work, we report the synthesis of *N*-cyanoethyl polyethylenimine (CN-PEI) with different cyanoethylation levels by modifying PEI with acrylonitrile (AN) through a Michael addition reaction. The adhesion capability of CN-PEI was characterized by peeling test. The electrochemical performances of LFP cathode with CN-PEI binder were systematically investigated by galvanostatic charge/discharge test, cyclic voltammetry and electrochemical impedance spectroscopy measurement.

Experimental

Synthesis and characterization of CN-PEI

CN-PEI was synthesized by modifying polyethylenimine with acrylonitrile (AN) through a Michael addition reaction. Polyethylenimine (PEI) (Mw = 70000 g mol^{-1}) was purchased from Aladdin Chemistry Co. (China). The purchased acrylonitrile (Xiya, Shandong, China; 99%) was purified by the distillation, and other chemicals were utilized as received. The steps of synthesis of CN-PEI can be described as follows:

In a two-necked glass reactor equipped with a magnetic stirrer and condenser, 1.00 g PEI was dissolved in 20 ml deionized water and stirred for 60 min under the condition of argon gas to remove oxygen. AN was added using injection and then stirred for 12 h at 60 °C. After reaction, the reacted system was dried at room temperature and formed a highly flexible film after 24 h. According to the [N]-to-[AN] ratio defined as the number of moles of the PEI repeating units,–(CH_2CH_2NH)–, divided by the number of moles of the AN, a series of CN-PEI were prepared at molar ratios of 10:5, 10:6, 10:7 and 10:8 and were defined as CN-PEI-5, CN-PEI-6, CN-PEI-7 and CN-PEI-8, respectively.

The chemical structures of CN-PEIs were confirmed by FT-IR measurement which was taken on a TENSOR27 spectrometer (Bruker, Germany) from 400 to 4000 cm^{-1} at the resolution of 4 cm^{-1}. The cyanoethylation modification degrees of CN-PEIs were analyzed by ^1H NMR using D_2O as a solvent on a Bruker AVANCE 600 spectrometer. Here the results of ^1H NMR and FT-IR for CN-PEI-7 are taken as an example:

FT-IR: 2252 cm^{-1} (–C≡N stretch), 3455 cm^{-1} (N–H stretch), 2923–2867 cm^{-1} (C–H stretch), 1680–1550 cm^{-1} (N–H bend).
^1H NMR (600 MHz, D_2O): δ 2.90–2.75 (–CH_2CN, br), 2.70–2.48 (–CH_2CH_2N, br), 2.60–2.48 (–NCH_2-CH_2CN, br).

For comparison, ^1H NMR and FT-IR for PEI are listed as follows:

FT-IR: 3455 cm^{-1} (N–H stretch), 2923–2867 cm^{-1} (C–H stretch), 1680–1550 cm^{-1} (N–H bend).
^1H NMR (600 MHz, D_2O): 2.70–2.48 (–CH_2CH_2N, br).

The cyanoethylation modification degree was analyzed by ^1H NMR from the ratio between the peaks of –CH_2CH_2N (δ 2.7–2.48 ppm) and –CH_2-CH_2CN (δ 2.90–2.7, 2.60–2.48 ppm). The modification degree was expressed as a number of modifications per repeating unit of PEI × 100%.

The distributions of droplet size for CN-PEIs were tested by dynamic light scattering (Zeta sizer Nano ZS, Malvern, English).

Physicochemical property

Adhesion strength of CN-PEIs, PEI and PVDF films coated onto the Al foil was measured using 180° high-precision micro-mechanical peel tester from Shenzhen Kaiqiangli testing instruments Co. (China) with the constant displacement rate of 20.0 mm min^{-1}. PVDF binder was used as the control sample for comparison. PVDF (Solvay Solef 16020) was purchased from Shenzhen Micro Electro Co. (China).

The swelling property of the binder with the electrolyte was examined by a swelling test. Binder sheets were prepared by solution-cast samples, and the solvents were removed in a vacuum oven at 60 °C overnight. Binder sheets were then placed in the electrolyte at room temperature for 48 h. The swelling ratio was defined as the weight ratio of the amount of absorbed solvent to the dry weight of the tested binder sheet. The electrolyte of 1 M $LiPF_6$ in ethylene carbonate (EC, ≥ 99%)/diethylene carbonate (DEC, ≥ 99%)/dimethyl carbonate (DMC, ≥ 99%) (v/v/v = 1/1/1) was purchased from Zhangjiagang Guotai-Huarong New Chemical Materials Co. (China) (water content < 10 ppm).

Thermal gravimetric analysis (TGA) measurement was taken on a STA 409 C/PC-PFEIFFER VACUUMTGA-7 analyzer (NETZSCH-GertebauGmbH, Germany) in a nitrogen atmosphere with a heating rate of 10 °C min^{-1} from 25 to 800 °C.

Electrode preparation

The electrode was fabricated using a typical slurry coating method. The LFP powder, acetylene black (AB) and polymer binder in a mass ratio of 80:13:7 were dispersed in corresponding solvent (PEI and CN-PEI-7 in deionized water, PVDF in NMP). LFP powders were obtained from Shenzhen Dynanonic Co. (China) claimed in an average particle size of 350 nm. Acetylene black (AB) was purchased from Guangzhou Lithium Force Energy Co. (China). NMP (anhydrous, 99.5%) was purchased from Aldrich. The slurry was coated onto a 20-μm-thick Al foil and then dried at 110 °C in a vacuum oven for 24 h to remove the solvent thoroughly.

Electrochemical measurement

In order to test the electrochemical stability of the CN-PEI-7, CN-PEI-7 was coated onto the Al foil and dried in vacuum for 12 h at 110 °C. Then it was pouched into a circular size of 14 mm. The CR2025-type coin cell was assembled in an argon-filled glove box using the electrode with CN-PEI-7, Celgard 2300 film as separator and lithium foil as counting electrode. The cell was measured by cyclic voltammetry test carried out between 2.5 and 4.0 V with a scanning rate of 0.2 mV s^{-1} on a Zennium/IM6 electrochemical workstation (Zahner, Germany).

The charge–discharge measurements were taken using CR2025-type coin cells. The diameter of the electrode was 14 mm, and the mass loading of active material was kept at 4.0 ± 0.2 mg. The CR2025-type coin cells were assembled in an argon-filled glove box using a lithium foil as counter electrode, Celgard 2300 film as separator. The cells were charged and discharged galvanostatically between 2.5 and 4.0 V at 25 °C on multi-channels battery tester (NEWARE, Shenzhen, China).

Cyclic voltammetry (CV) was conducted using an electrochemical workstation (Zahner, Germany) at a scan rate of 0.2 mV s^{-1} from 2.5 to 4.0 V. Electrochemical impedance spectroscopy (EIS) was measured by applying an alternating voltage of 5 mV over the frequency ranging from 10^{-2} to 10^{5} Hz using an electrochemical workstation (Zahner, Germany). The morphologies of LFP electrodes with different binders were observed by scanning electron microscopy (SEM; Hitachi S-4800, Japan).

To test the dispersion ability of CN-PEI-7 and PEI binder for the LFP aqueous slurry, agglomerate size and zeta potential measurements were investigated for LFP slurry on Zeta sizer Nano ZS (Malvern, English). The test sample was prepared by the following steps: Before coating, a small quantity of the LFP slurry was poured into a vial and added some DI water to adjust the concentration to 0.05% by weight. Then it was stirred magnetically for 24 h to obtain a LFP–AB suspensions allowing adequate time for charge adsorption and desorption on the LFP/AB particle surfaces to reach equilibrium.

To testify the complexation between lithium ions and the polar cyano group, FT-IR measurements of CN-PEI-7:$LiPF_6$ samples were tested on a TENSOR27 spectrometer (Bruker, Germany) from 400 to 4000 cm^{-1} at the resolution of 4 cm^{-1}. CN-PEI-

7:$LiPF_6$ samples were prepared by first dissolving CN-PEI-7 and $LiFP_6$ (Aldrich) in anhydrous acetonitrile (Aldrich) in the desired [N]-to-[Li^+] (molar) ratios. The [N]-to-[Li^+] ratio is defined as the number of moles of the PEI repeating units, –(CH_2CH_2NH)-, divided by the number of moles of the $LiPF_6$. Solutions of the CN-PEI-7:$LiPF_6$ samples were cast on KBr salt plates, and acetonitrile was evaporated over 48 h in a continuous purge dry box, leaving a thin polymer electrolyte film.

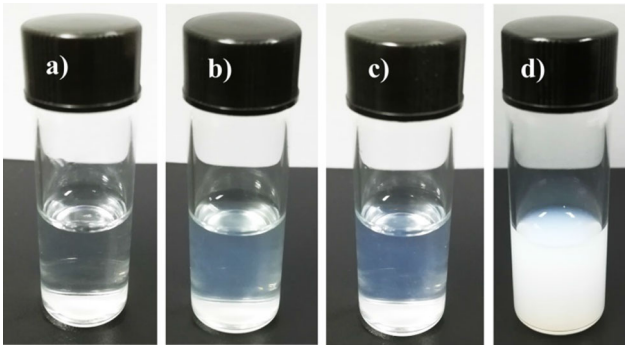

Figure 1 Photographs of CN-PEIs with different cyanoethylation levels: CN-PEI-5 (**a**), CN-PEI-6 (**b**), CN-PEI-7 (**c**), CN-PEI-8 (**d**).

Results and discussion

Synthesis and characterization of CN-PEI

Scheme 1 shows the synthesis of CN-PEI. AN reacts with the primary amine and secondary amine of PEI through a Michael addition reaction. By controlling the feeding ratio of AN, a series of CN-PEIs were synthesized. Depending on the cyanoethylation level, CN-PEI was obtained as a form of transparent solution, bluish micro-emulsion or turbid emulsion in water (Fig. 1). As shown in Fig. S1, the highly flexible CN-PEI polymer was obtained upon cyanoethylation.

The chemical structures of CN-PEIs and PEI were identified by ^{1}H NMR spectrum (Fig. S2) and FT-IR spectrum (Fig. 2a). The ^{1}H NMR spectrum of CN-PEI shows new peak at δ 2.90–2.75 ppm corresponding to the –CH_2CN and the peak of -NCH_2CH_2CN at δ 2.60–2.48 ppm overlapping with the peak –CH_2CH_2N (2.70–2.48 ppm) [15]. An intensive peak for –C≡N bond at 2252 cm^{-1} for CN-PEI is detected in FT-IR spectrum after the cyanoethylation of PEI. These results indicate the successful cyanoethylation of PEI. The modification degree was analyzed by ^{1}H NMR [Eq. (1)].

$$m = \frac{2}{n-1} \times 100\% \quad (1)$$

where n is integration of the peaks of CN-PEI (δ 2.7–2.48 ppm)/integration of the peaks of CN-PEI (δ 2.75–2.9 ppm) in ^{1}H NMR spectrum of CN-PEI. In our experiment, the modification degrees of different CN-PEIs are shown in Table 1.

The distributions of droplet size for CN-PEI-6/7/8 were tested by dynamic light scattering to further demonstrate the formation of micro-emulsion and emulsion (Fig. S3). With the increase in cyanoethylation level, the Z-average diameter (Dz) of droplet size for CN-PEI increases. The Z-average diameter for CN-PEI-6, CN-PEI-7 is 55.2 and 64.8 nm, respectively. This favors the formation of micro-emulsion [16]. CN-PEI-6 and CN-PEI-7 also display a typical bluish color of micro-emulsion system. CN-PEI-8 with high cyanoethylation level shows a Z-average diameter of 259.1 nm and becomes a turbid emulsion (Dz > 100 nm). CN-PEI-8 precipitates without stirring after 2 h and is not suitable to be a water-soluble binder.

Physicochemical property

To evaluate the adhesion capability of different binders, peeling tests for CN-PEIs, PEI and PVDF were conducted (Fig. 2b). CN-PEI-7 shows the highest adhesion strength (1.73 N cm^{-1}) than that of PVDF

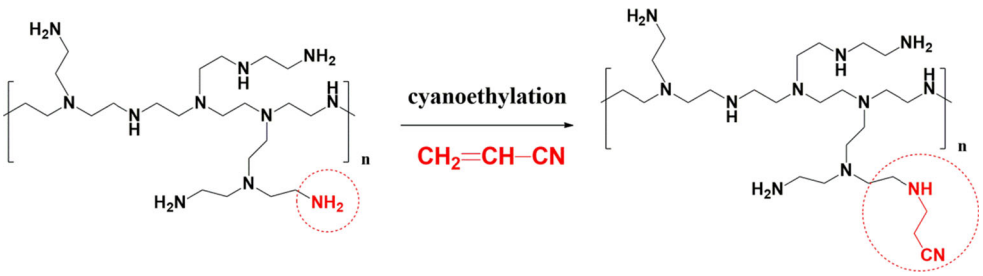

Scheme 1 Schematic route of CN-PEI synthesis (acrylonitrile can react with the primary amine and secondary amine of PEI through a Michael addition reaction).

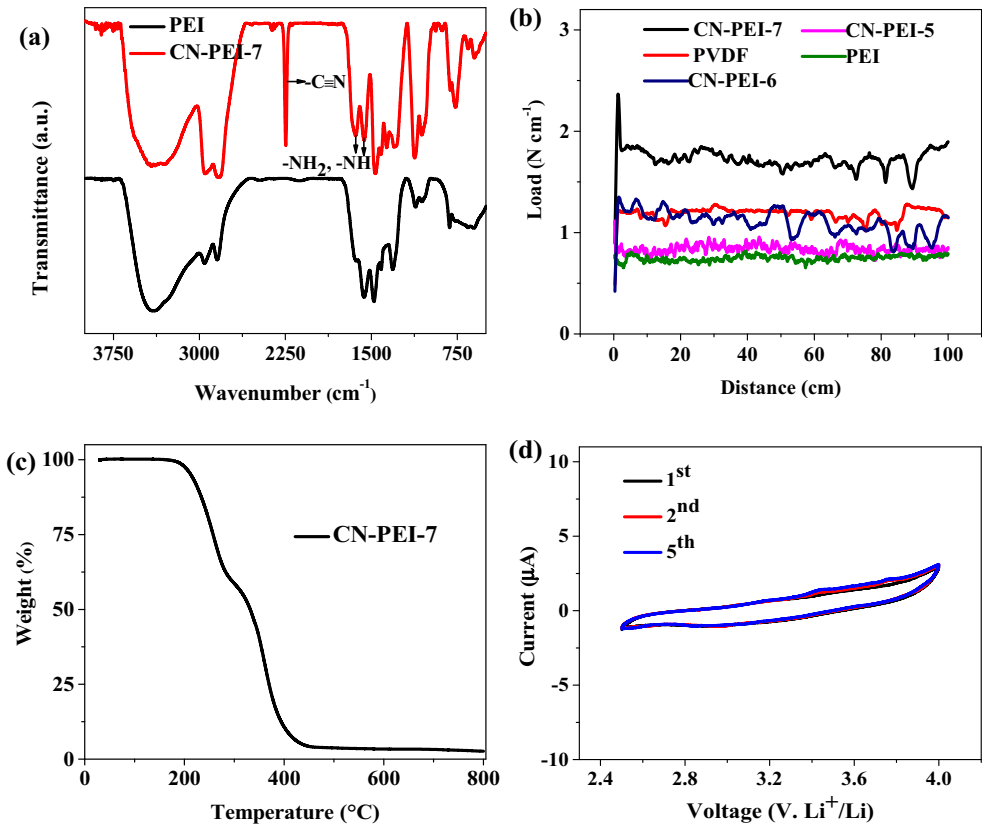

Figure 2 FT-IR spectra of PEI and CN-PEI-7 (**a**), peeling test profiles of different binders (**b**), TGA plot of CN-PEI-7 (**c**), CV measurement of CN-PEI-7 binder (**d**).

Table 1 Z-average diameter of droplet size and cyanoethylation modification degree for CN-PEIs

	CN-PEI-5	CN-PEI-6	CN-PEI-7	CN-PEI-8
Modification degree (%)	48	55	67	76
Dz (nm)	–	55.2	64.8	259.1

(1.24 N cm^{-1}) and PEI (0.73 N cm^{-1}). Apparently the cyanoethylation can improve adhesion strength of PEI. CN-PEI possesses the cyano group which has a stronger polarity than amine group interacting more strongly with their environments by hydrogen bonding and dipole–dipole interactions [17]. As a result, CN-PEI shows an improvement in adhesion strength than PEI.

In this study, we focused on CN-PEI-7 binder as a water-soluble binder for LFP cathode because it shows the best adhesion ability.

The swelling property of the binder with the electrolyte was examined by a swelling test. The swelling ratio of CN-PEI-7 has a smallest value of 10.34% as compared with 23.13 and 22.67% for PEI and PVDF, respectively, indicating that CN-PEI-7 is more resistant in the electrolyte. It can help maintain the stability of LFP electrode's structure and is favorable for long-term cycling than PEI and PVDF.

The thermal stability for CN-PEI-7 was tested by TGA measurement (Fig. 2c). The steep curve shows the carbonization process with the initiation temperature of 182.7 °C. It indicates CN-PEI-7 can maintain its thermal stability during the slurry preparation and electrode fabrication ($T < 120$ °C).

Electrochemical performance

The electrochemical behavior of CN-PEI-7 is evaluated through cyclic voltammetry (CV) (Fig. 2d). The CV profile demonstrates that CN-PEI-7 is electrochemically stable in the cathode working voltage range of 2.5–4.0 V. This inert electrochemical property during the 2.5–4.0 V range guarantees that the

CN-PEI-7 binder will not impede the lithiation/delithiation processes.

The cycle performances of LFP electrodes with different binders at C/2 were investigated (Fig. 3). As shown in Fig. 3a, LFP electrode with CN-PEI-7 binder delivers an initial discharge capacity of 149 mAh g^{-1} and achieved capacity retention of 99.6% after 100 cycles, while LFP electrode with PVDF exhibits an initial discharge capacity of 148.7 mAh g^{-1} and 97.3% capacity retention after 100 cycles of charge/discharge. LFP electrode with PEI is worse exhibiting an initial discharge capacity of 138.9 mAh g^{-1} and 94.5% capacity retention after 100 cycles of charge/discharge.

The discharge/charge curves of LFP electrodes with different binders from 1st to 100th cycle are employed to further investigate and understand the differences in cycle performance. An obvious capacity degradation and voltage fading from 1st to 100th cycle can be observed for LFP electrode with PVDF and PEI compared to CN-PEI-7. Gap between discharge and charge plateaus (ΔE) indicates that the polarization of the electrode is related to their electrode impedances, which is largely affected by the interface performance (interface stability and interface resistance for ion/electron transfer) among active materials, conductive materials and the current collector. ΔE widens slightly for LFP electrode with CN-PEI-7 compared to PVDF or PEI. To demonstrate this further, Fig. S4 shows the charge/discharge curves of LFP electrodes with different binders at the 1st cycle and 100th cycle, respectively. LFP electrode with CN-PEI-7 shows the smallest polarization of 63 mV at the 1st cycle and still maintains 64 mV after 100 cycles of charge/discharge, suggesting the fast redox kinetics and good cycle stability.

Figure 4 shows the rate performances of LFP electrodes with different binders. The rate test was increased gradually from C/10 to 5 C and finally returned to C/10. LFP electrode delivers an initial discharge specific capacity of 164.4, 158.2, 146.8 mAh g^{-1} at C/10 with CN-PEI-7, PVDF and PEI, respectively. Upon increasing the charge/discharge rate, better electrochemical performances for LFP electrode with CN-PEI-7 are found. At 2 C, LFP electrode delivers a discharge specific capacity of

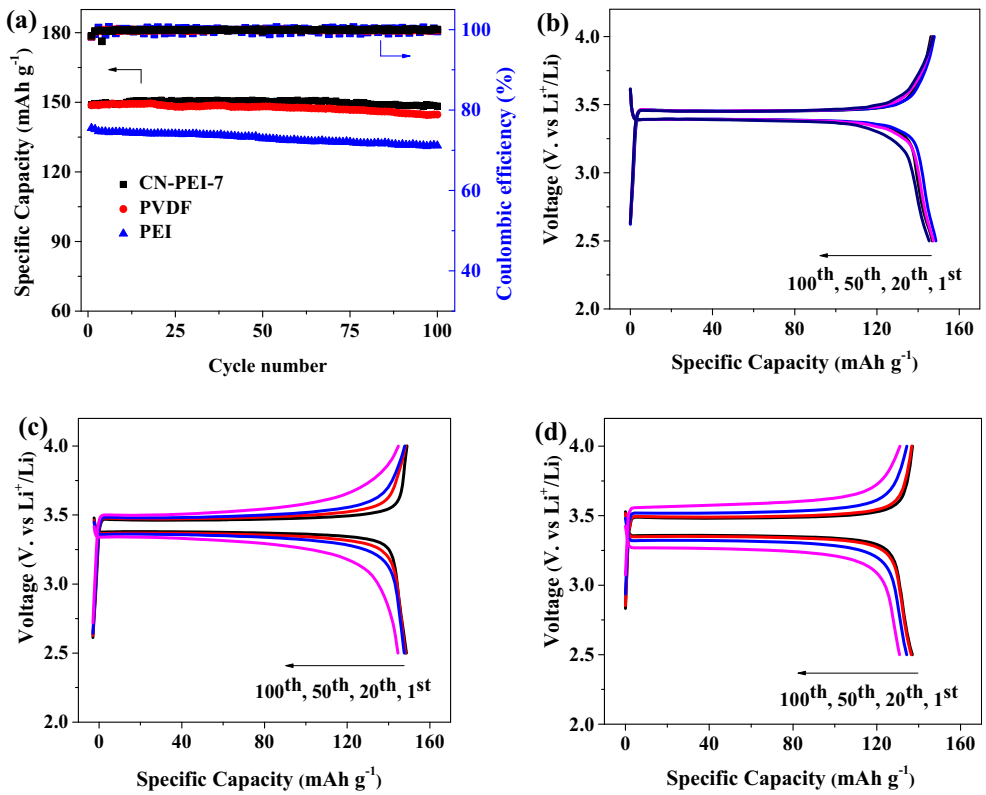

Figure 3 Cycle performances (**a**) at C/2 of LFP electrodes with different binders. Discharge curves at C/2 for LFP electrode with CN-PEI-7 (**b**), PVDF (**c**) or PEI (**d**) binder.

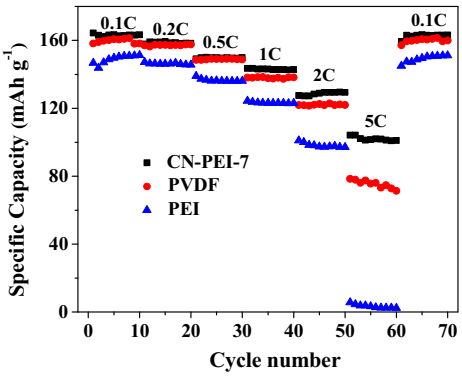

Figure 4 Rate performances of LFP electrodes with different binders.

128.9, 121.9 and 98 mAh g^{-1} with CN-PEI-7, PVDF and PEI, respectively. When the current density is increased to 5 C, LFP electrode with CN-PEI-7 shows a much higher discharge capacity of 102.4 mAh g^{-1} retaining 62.3% discharge capacity of its C/10 capacity, as compared with 53.1 and 3.88% for PVDF and PEI, respectively. When the rate is returned to C/10, the reversible discharge capacity rapidly increases to 159.4, 157.2 and 145 mAh g^{-1} for LFP electrode with CN-PEI-7, PVDF and PEI, respectively. This result demonstrates that the LFP electrode with CN-PEI-7 has an excellent reversibility and stability. Through the above-mentioned results, LFP electrode with CN-PEI-7 shows much better rate capability than PVDF or PEI.

To understand the above electrochemical performances, surface morphologies of LFP electrodes with different binders were obtained using SEM. Figure 5 shows the SEM images of LFP electrode before and after 100 cycles with CN-PEI-7, PVDF and PEI, respectively. Before cycling, the LFP and AB particles of the LFP electrode are homogeneously mixed together using the CN-PEI-7, PVDF or PEI. It indicates that CN-PEI-7 can exhibit a good dispersion for LFP slurry under aqueous condition. Some LFP agglomerates and surficial protrusions can be observed after 100 cycles in LFP electrode with CN-PEI-7, PVDF or PEI, which is unfavorable for the electrolyte to permeate into the internal of active materials and decreases the channel for Li^+ transportation. But the situation of LFP electrode with CN-PEI-7 is much slighter comparing to PVDF and PEI where many LFP particles were linked together to be a very big block. This benefits from the good adhesion strength that CN-PEI-7 provides guaranteeing interface stability over the process of charge and discharge. As a result, LFP electrode with CN-PEI-7 delivers high capacity and superior cycling stability.

Replacing NMP with water creates problem with dispersion stability due to hydrogen bonding and strong electrostatic forces, especially when nano-/micro-sized materials are involved [18]. To minimize agglomeration, the key is to increase the repulsive potential (i.e., increase the Coulomb force) between particles. Agglomerate size and zeta potential measurements for LFP slurry were tested to understand the mechanism of the dispersion ability of CN-PEI-7.

Figure S5(a, b) shows the distribution of the agglomerate size for LFP slurry with CN-PEI-7 and PEI, respectively. The Z-average diameter for LFP slurry with CN-PEI-7, PEI is 343 and 358 nm, respectively, which is in accordance with the particle size of LFP used in our experiment. And from the distribution, it can be seen that there is no bulky grain caused by the agglomeration of the particle of LFPs/ABs. To further demonstrate the mechanism of the dispersion ability, the zeta potential for LFP slurry using CN-PEI-7 and PEI is shown in Fig. 6. LFP aqueous slurry with CN-PEI-7 or PEI yields a positive charge. It indicates that the CN-PEI-7 or PEI polymer with positive charge caused by the protonation of amine group under aqueous condition successfully adsorbs on the surface of LFP/AB particles. Figure S5c shows the schematic illustration of dispersion mechanism. These findings can further illustrate the CN-PEI-7 can disperse LFP/AB particles effectively under aqueous condition reducing the happening of agglomeration and further keep the efficiency of the active materials.

It has been identified that CN-PEI-7 binder could effectively maintain the structural integrity and morphology of electrode as well, leading to improved electrochemical performance. To further investigate the electrochemical kinetics, CV measurements and the electrochemical impedance spectroscopy (EIS) measurements of LFP electrodes with different binders were taken. CV measurement was taken at a scan rate of 0.2 mV s^{-1} from 2.5 to 4.0 V (Fig. 7a). A single pair of oxidation and reduction peaks (around 3.6 and 3.3 V), which corresponds to Fe^{3+}/Fe^{2+} redox couple, is observed for all of binder systems. The potential intervals between the oxidation and the reduction peak are 0.32, 0.55 and 0.71 V for CN-PEI-7, PVDF and PEI, respectively. Meanwhile, LFP electrode with CN-PEI-7 shows sharper anodic and

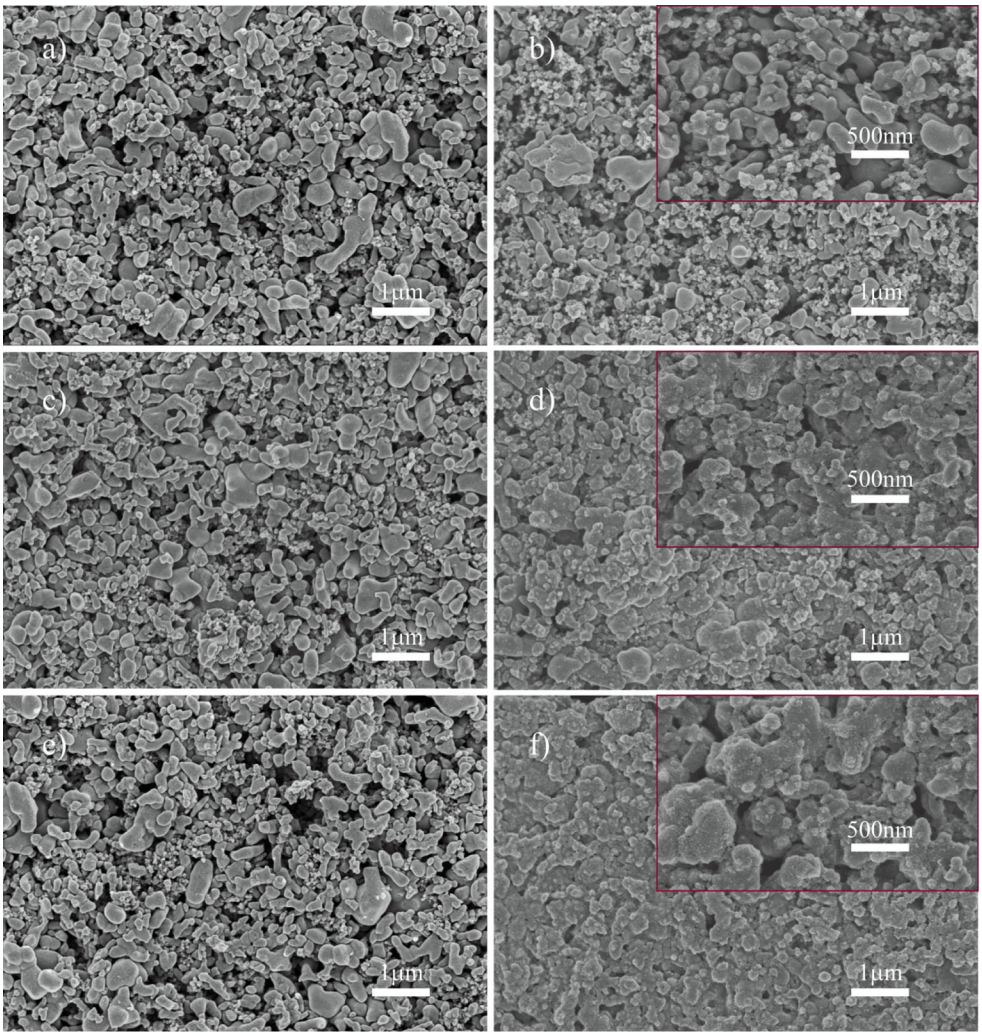

Figure 5 SEM images of LFP electrodes with different binders, (**a**, **c**, **e**) before and (**b**, **d**, **f**) after 100-cycle charge–discharge test: **a**, **b** CN-PEI-7, **c**, **d** PVDF and **e**, **f** PEI binder, respectively.

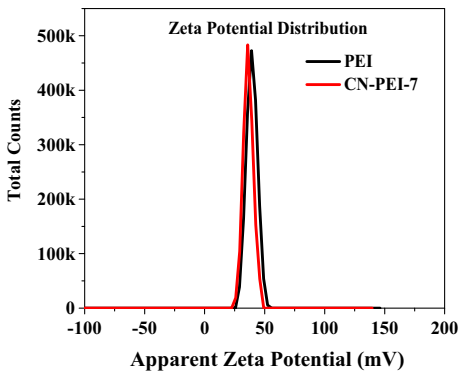

Figure 6 Zeta potential for LFP slurry with CN-PEI-7 and PEI.

cathodic peaks than PVDF or PEI and the current of the peak for LFP electrode with CN-PEI-7 is the largest. The above-mentioned results demonstrate that LFP electrode with CN-PEI-7 has a lower polarization and favorable electrochemical kinetics than PVDF or PEI, which is consistent with the electrochemical results.

The improvement in the interface performance can be quantitatively evaluated by EIS measurements. Figure 7b shows the Nyquist curves of the electrodes with different binders in the discharged state of 3.5 V (vs. Li/Li^+) at room temperature after 3 cycles. All the EIS spectra are composed of a semicircle and a sloping line. The obtained spectra are fitted using Zview software according to the equivalent circuit in the inset of Fig. 7b, where R_e is the resistance of electrolyte, CPE as the constant phase element of the double layer capacity, R_{ct} is the charger-transfer

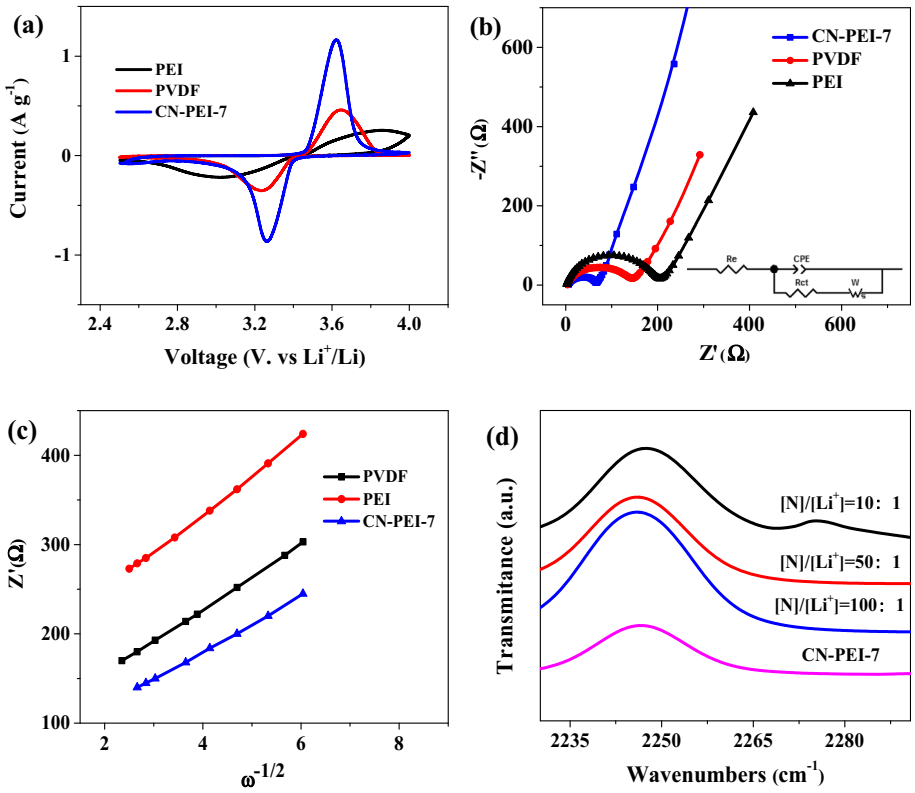

Figure 7 CV profile (**a**), Nyquist curves (**b**), Warburg plots (**c**) of LFP electrodes with different binders. FT-IR spectra of CN-PEI-7:$LiPF_6$ at 10:1, 50:1 and 100:1 compositions and pure CN-PEI-7 in the (C≡N) region (**d**).

resistance and W is the Warburg impedance related to Li^+ diffusion.

The Warburg coefficient (σ_w) can be calculated by Eq 2: [19]

$$Z' = R_e + R_{ct} + \sigma_w \cdot \omega^{-1/2} \quad (2)$$

The Warburg plots in the low-frequency region are shown in Fig. 7c. The slope of the fitted line is the Warburg coefficient σ_w. The calculated value of σ_w for CN-PEI-7, PVDF and PEI is 30.807, 36.046 and 42.5, respectively (Table S1). Diffusion coefficient of lithium ion (D_{Li}) is inversely proportional to Warburg coefficient σ_w as shown in Eq 3: [19]

$$D_{Li} = \frac{R^2T^2}{2n^4F^2c^2\sigma^2} \quad (3)$$

where R and T are the gas constant and temperature, respectively, and n and F are the charge transfer number and Faraday constant, respectively. c and σ are concentration of lithium and Warburg coefficient, respectively. It can be easily found LFP electrode with CN-PEI-7 has the largest D_{Li} among the three electrodes, which is favorable for rapid charge and discharge.

The EIS results are listed in Table S1. All the binders share similar R_e values due to the use of identical electrolyte solution. In contrast, the R_{ct} of LFP electrode with CN-PEI-7 is significantly lower than PVDF and PEI, exhibiting 64.19, 142.6 and 200 Ω, respectively. From the mentioned above, it is seen that LFP electrode with CN-PEI-7 exhibits the largest D_{Li} and lowest R_{ct} exhibiting a favorable electrochemical kinetics. This benefits from the excellent adhesion strength of CN-PEI-7 and uniform dispersion of LFP/AB particles in the electrode. It effectively guarantees the structural integrity and morphology of the electrode over the process of charge and discharge. In addition, cyano groups provide complexation sites with lithium ions and thus transport pathways for lithium ions, leading to CN-PEI-7 binder with higher ionic conductivity [20, 21]. The higher ionic conductivity decreases the polarization and impedance of LFP electrode, and supports a favorable electrochemical kinetic.

To testify the complexation between lithium ions and the polar cyano group, FT-IR measurements of CN-PEI-7:$LiPF_6$ samples were taken. It has been demonstrated by several groups that a higher-frequency shoulder than the free (C≡N) band at 2252 cm^{-1} is present in PAN:LiTf samples at high LiTf concentrations and has been attributed to nitrile

complexation with Li^+ [22, 23]. To see the complexation more obviously, different [N]-to-[Li^+] ratios of CN-PEI-7:$LiPF_6$ samples were tested. It is seen that at salt concentrations of 10:1, an obvious higher-frequency shoulder on the CN-PEI-7 versus (C≡N) band develops (Fig. 7d). This implies that the complexation between lithium ions and the polar cyano group happens. As a result, it provides an improvement in the ionic conductivity for CN-PEI-7.

Conclusions

In summary, CN-PEI is successfully synthesized by modifying PEI with AN through a Michael addition reaction. By controlling cyanoethylation level, CN-PEI can be obtained as a form of solution, microemulsion or emulsion in water. CN-PEI microemulsion is investigated as water-soluble binder for the application of LFP cathode in lithium-ion batteries. CN-PEI binder not only maintains the outstanding dispersion capability of PEI but also exhibits an excellent adhesion strength and higher ionic conductivity because of the introduction of polar cyano groups. As a result, CN-PEI binder can effectively maintain the mechanical integrity and decrease the polarization of LFP electrode during the operation of the battery. LFP electrode with CN-PEI binder exhibits good cycle stability and enhanced rate performance. Overall, we provide a new water-soluble CN-PEI binder and comprehensive understanding of the working mechanism of CN-PEI as binder for LFP cathode from structural to electrochemical aspects and further develop the LFP cathode materials for high-performance lithium-ion batteries.

Acknowledgements

This work was supported by the K.C. Wong Education Foundation, National Natural Science Foundation of China (21573239), Science & Technology project of Guangdong Province (2014TX01N014/2015B010135008), Guangzhou Municipal Project for Science & Technology (201509010018).

Compliance with ethical standards

Conflict of interest The authors declare that they have no conflict of interest.

Electronic supplementary material: The online version of this article (https://doi.org/10.1007/s10853-018-2247-y) contains supplementary material, which is available to authorized users.

References

[1] Li GR, Ling M, Ye YF, Li ZP, Guo JH, Yao YF, Zhu JF, Lin Z, Zhang SQ (2015) Acacia senegal-inspired bifunctional binder for longevity of lithium–sulfur batteries. Adv Energy Mater 5(21):1500878

[2] Li C-C, Lin Y-S (2012) Interactions between organic additives and active powders in water-based lithium iron phosphate electrode slurries. J Power Sources 220:413–421

[3] Wang QS, Ping P, Zhao XJ, Chu GQ, Sun JH, Chen CH (2012) Thermal runaway caused fire and explosion of lithium ion battery. J Power Sources 208:210–224

[4] Ryou MH, Kim J, Lee I, Kim S, Jeong YK, Hong S, Ryu JH, Kim TS, Park JK, Lee H, Choi JW (2013) Mussel-inspired adhesive binders for high-performance silicon nanoparticle anodes in lithium-ion batteries. Adv Mater 25(11):1571–1576

[5] Kovalenko I, Zdyrko B, Magasinski A, Hertzberg B, Milicev Z, Burtovyy R, Luzinov I, Yushin G (2011) A major constituent of brown algae for use in high-capacity Li-ion batteries. Science 334(6052):75–79

[6] Buqa H, Holzapfel M, Krumeich F, Veit C, Novak P (2006) Study of styrene butadiene rubber and sodium methyl cellulose as binder for negative electrodes in lithium-ion batteries. J Power Sources 161(1):617–622

[7] Yue L, Zhang LZ, Zhong HX (2014) Carboxymethyl chitosan: a new water soluble binder for Si anode of Li-ion batteries. J Power Sources 247:327–331

[8] Zhong H, Zhou P, Yue L, Tang D, Zhang L (2014) Micro/-nano-structured SnS_2 negative electrodes using chitosan derivatives as water-soluble binders for Li-ion batteries. J Appl Electrochem 44(1):45–51

[9] Sun MH, Zhong HX, Jiao SR, Shao HQ, Zhang LZ (2014) Investigation on carboxymethyl chitosan as new water soluble binder for LiFePO4 cathode in Li-ion batteries. Electrochim Acta 127:239–244

[10] Zhong H, He A, Lu J, Sun M, He J, Zhang L (2016) Carboxymethyl chitosan/conducting polymer as water-soluble composite binder for LiFePO4 cathode in lithium ion batteries. J Power Sources 336:107–114

[11] He JR, Wang JL, Zhong HX, Ding JN, Zhang LZ (2015) Cyanoethylated carboxymethyl chitosan as water soluble binder with enhanced adhesion capability and

electrochemical performances for LiFePO4 cathode. Electrochim Acta 182:900–907

[12] Li JL, Armstrong BL, Kiggans J, Daniel C, Wood DL (2012) Optimization of LiFePO4 nanoparticle suspensions with polyethyleneimine for aqueous processing. Langmuir 28(8):3783–3790

[13] Bae J, Cha SH, Park J (2013) A new polymeric binder for silicon-carbon nanotube composites in lithium ion battery. Macromol Res 21(7):826–831

[14] Chen W, Qian T, Xiong J, Xu N, Liu XJ, Liu J, Zhou JQ, Shen XW, Yang TZ, Chen Y, Yan CL (2017) A new type of multifunctional polar binder: toward practical application of high energy lithium sulfur batteries. Adv Mater 29(12):1605160

[15] Erickson M, Frech R, Glatzhofer DT (2003) Solid polymer/salt electrolytes based on linear poly ((N-2-cyanoethyl) ethylenimine). Electrochim Acta 48(14–16):2059–2063

[16] Slomkowski S, Alemán JV, Gilbert RG, Hess M, Horie K, Jones RG, Kubisa P, Meisel I, Mormann W, Penczek S, Stepto RFT (2011) Terminology of polymers and polymerization processes in dispersed systems (IUPAC Recommendations 2011). Pure Appl Chem 83(12):2229–2259

[17] Gong L, Nguyen MHT, Oh E-S (2013) High polar polyacrylonitrile as a potential binder for negative electrodes in lithium ion batteries. Electrochem Commun 29:45–47

[18] Li J, Armstrong BL, Kiggans J, Daniel C, Wood DL 3rd (2012) Optimization of LiFePO4 nanoparticle suspensions with polyethyleneimine for aqueous processing. Langmuir 28(8):3783–3790

[19] Ling M, Qiu JX, Li S, Yan C, Kiefel MJ, Liu G, Zhang SQ (2015) Multifunctional SA-PProDOT binder for lithium ion batteries. Nano Lett 15(7):4440–4447

[20] Mathews KL, Budgin AM, Beeram S, Joenathan AT, Stein BD, Werner-Zwanziger U, Pink M, Baker LA, Mahmoud WE, Carini JP, Bronstein LM (2013) Solid polymer electrolytes which contain tricoordinate boron for enhanced conductivity and transference numbers. J Mater Chem A 1(4):1108–1116

[21] Luo L, Xu Y, Zhang H, Han X, Dong H, Xu X, Chen C, Zhang Y, Lin J (2016) Comprehensive understanding of high polar polyacrylonitrile as an effective binder for Li-ion Battery nano-Si anodes. ACS Appl Mater Interfaces 8(12):8154–8161

[22] Wang ZX, Huang BY, Huang H, Chen LQ, Xue RJ, Wang FS (1996) Investigation of the position of Li + ions in a polyacrylonitrile-based electrolyte by Raman and infrared spectroscopy. Electrochim Acta 41(9):1443–1446

[23] Ferry A, Edman L, Forsyth M, MacFarlane DR, Sun JZ (2000) NMR and Raman studies of a novel fast-ion-conducting polymer-in-salt electrolyte based on LiCF3SO3 and PAN. Electrochim Acta 45(8–9):1237–1242